Journal of Non-Crystalline Solids 356 (2010) 911–916

Contents lists available at ScienceDirect

Journal of Non-Crystalline Solids

journal homepage: www.elsevier.com/locate/jnoncrysol

Indium tin oxide thin films for silicon-based electro-luminescence devices prepared by electron beam evaporation method

Neng Wan, Tao Wang, Hongcheng Sun, Guran Chen, Lei Geng, Xinhui Gan, Sihua Guo, Jun Xu *, Ling Xu, Kunji Chen

Nanjing National Laboratory of Microstructures, Jiangsu Provincial Key Laboratory of Photonic and Electronic Materials Sciences and Technology, School of Physics and School of Electronic Science and Technology, Nanjing University, Nanjing 210093, PR China

ARTICLE INFO

Article history:
Received 26 March 2009
Received in revised form 17 December 2009
Available online 18 January 2010

Keywords:
Electrical and electronic properties
Films and coatings
Electroluminescence
Indium tin oxide and other transparent conductors

ABSTRACT

Tin doped indium oxide thin films were deposited by electron beam evaporation (EBE) method. The influences of deposition atmosphere, film thickness and post-annealing temperature on the optical and electrical properties are studied. It is found that depositing films in oxygen atmosphere is helpful for improving the electrical and optical performance due to the improvement of the film microstructure. The sheet resistance is increased obviously in ITO films with reducing the film thickness, which is caused by the enhanced surface scattering towards the carriers. The obtained ITO thin films deposited under optimized conditions have good electrical and optical properties with typical resistivity of $4.5 \times 10^{-4}\ \Omega$ cm and the optical transmittance of about 85% (at 550 nm). Furthermore, the EBE deposited ITO thin film can be applied as the top electrode in the Si-based electro-luminescence devices and a strong electro-luminescence (EL) is observed.

© 2010 Elsevier B.V. All rights reserved.

1. Introduction

Tin doped indium oxide (ITO) has been used in many kinds of advanced opto-electronic devices due to its unique properties [1–3]. The un-doped indium oxide is n-type semiconductor with a fundamental band-gap of 3.65 eV. By doping with tin, the density of the carrier can be increased up to the Mott critical ($\sim 10^{20}$/cm^3), and the highly degenerated semiconductor is formed [1]. This highly doped semiconductor is characterized as high transparency in visible light region, high reflection in infrared region, strong absorption in UV region and high conductivity at room temperature. ITO films can be used in many fields, such as smart windows for energy saving due to its high reflection in the infrared region and high transmission in visual region [1], and transparent conduction oxide (TCO) electrode in solar cells and electro-luminescence (EL) devices due to its high conductance and transmission in wide optical range [2,3].

So far, many methods have been used to deposit ITO thin films, such as pulsed laser deposition (PLD) [4,5], sputtering [6], e-beam evaporation (EBE) [7], sol–gel technique [8], and spray pyrolysis [9,10]. Among all these methods, e-beam evaporation has the advantages of low cost, low temperature, high purity and high deposition rate [1,7]. Motivated by the need of high transparency and high conduction of the ITO thin films in EL devices, it is interesting to study the influences of deposition parameters on the film properties in order to further understand the fundamental deposition process of ITO films. In this work, the e-beam evaporation method was used to deposit ITO thin films with low resistance and high transparency. The effect of oxygen pressure, substrate temperature, and annealing temperature on the electrical and optical properties were studied and correlated with each other. The optimized deposition parameters were discussed and concluded. ITO thin films deposited under the optimized deposition conditions show the good electrical and optical properties which is comparable with the best results of ITO films prepared by other different techniques. The performance of EL devices with the ITO top electrode on the Si/SiO_2 multilayer is experimentally demonstrated.

2. Experiments

ITO pellets of In/Sn = 95/5 filled in a copper crucible were used as evaporation sources. The electron beam source is the heated tungsten filament under an accelerating voltage of 6 kV. Glass slide with the dimension of 1 cm × 2 cm was used as substrate which is placed on a substrate holder. The substrate temperature is controlled by a heater attaching on the back of the substrate holder, and the distance from the substrate holder to the evaporation source is about 40 cm. During all the experiments the base pressure is lower than 5×10^{-4} Pa. In some of the deposition process, oxygen gas is introduced into the evaporation chamber by using a needle valve. The deposition rate and the thickness of the film

* Corresponding author.
E-mail address: junxu@nju.edu.cn (J. Xu).

0022-3093/$ - see front matter © 2010 Elsevier B.V. All rights reserved.
doi:10.1016/j.jnoncrysol.2009.12.026

is monitored and controlled through a quartz crystal probe assembled at the center of the substrate holder. The as-deposited films were annealed in a quartz tube furnace under N_2 atmosphere at different temperatures for half an hour in order to promote the crystallization and elevate the carrier concentration [8].

Various kinds of methods were used to characterize the microstructures and physical properties of ITO films. X-ray diffraction (XRD, Rigaku, D/Max-RA) method was employed for studying the crystal structure of the ITO films. Field emission scanning electron microscopy (FESEM, LEO 1530VP, Zeiss) was adopted for observing the surface morphology and measuring the thickness of the films. The In/Sn ratio in the film is determined by using the X-ray photoelectron spectroscopy (XPS, ESCALB MK-II) with the systematic error of 10% for determining the compositions in the film. UV/VIS/NIR transmission (T) and reflection (R) spectra were obtained by using Shimazu UV-3600 photospectrometer with the transmission measurement error less than 0.01%T and wavelength precision of 0.1 nm. The transmission spectra were obtained with air as reference in the normal incidence geometry, the reflection spectra were obtained with aluminum mirror as reference using a 5° reflection geometry, and the absorption (A) of the thin film is deduced by using the relationship of $A = 1 - R - T$. The resistance of the ITO films was measured by using the four probe method. The EL signals from ITO coated Si quantum dots-based devices were collected by using JY Fluromax-2 spectrometer at room temperature.

3. Results

It is well known that the deposition atmosphere has an important effect on the EBE process especially for depositing metal oxide materials and oxygen deficiency species will result in low transparency and poor optical and electric performance in the deposited ITO films [11,12]. Fig. 1(a) and (b) shows the FESEM micrographs of the ITO films deposited without oxygen and with the oxygen pressure of 2.7×10^{-2} Pa, respectively. The substrate temperature is kept at 150 °C during the deposition, and the thickness of the films is around 180 nm. It is found from the figures that the microstructure of the thin films is affected greatly by the oxygen gas. Films deposited without oxygen have porous structures. Some nanostructures with different sizes could be seen in the figure. Some of them are as large as 100 nm, while most of them are several tens of nanometers. A very different picture of surface morphology is observed with films deposited in oxygen rich atmosphere, which shows a condensed and flat surface. A lot of small grains could be observed in the figure, and the average grain size is about 30 nm with quite a good uniform size distribution. It is noted that the films annealed at different temperatures show similar microstructure with the as-deposited films, which could also be confirmed by the following XRD results.

The XRD patterns of the films deposited in oxygen atmosphere and post-annealed at different temperatures in N_2 are presented in Fig. 2. As seen in the figure, the as-deposited thin film shows relatively weaker XRD peaks indicating poor crystallization, while all the annealed ITO films are well crystallized into the BCC structure [6]. The intensity of diffraction peaks increases with elevating the annealing temperature, indicating that the crystallization of the thin film is improved after high temperature annealing. The full width at half maximum of the diffraction peaks decrease with elevating the annealing temperature, indicating the grain size increases with higher annealing temperature, which can be ascribed to the low crystallization temperature of ITO films.

Fig. 3(a)–(f) gives the optical transmission, reflection and absorption spectra of the film deposited without and with oxygen, respectively. As shown in the figures, the as-deposited films have low transmission during the whole range of the spectrum. Comparing with the films deposited without oxygen atmosphere, the films deposited in oxygen atmosphere show higher transmission, suggesting that the oxygen deficiency could be one of the sources for the low optical transmission. High temperature annealing is efficient for enhancing the transmission. As seen in the transmission spectra, the film annealed above 350 °C shows good transparency in the visual light region both for films deposited with (about 85% at 550 nm) or without oxygen gas (about 80% at 550 nm). We ascribe the improved optical transmission to the improvement of the film microstructure and elimination of the defects after high temperature annealing. The sharp falling-down in the transmission spectra below 400 nm is caused by the strong absorption of the glass substrate and ITO itself, because the band-gap of ITO is about 3.65 eV (~340 nm) and the glass substrate show strong absorption below 350 nm. This can also be easily interpreted from the absorption spectra shown in Fig. 3(c) and (f). A decrease in the infrared region (above 1600 nm) is observed in all of the transmission spectra, and this is mainly due to the high infrared reflection of the ITO films [1], which can be directly observed in Fig. 3(b) and (e). The reflection in the near infrared region can be ascribed to the carrier plasma generated by the high degeneration of the ITO thin films. According to the XPS results (not shown here) the films always have the stoichiometry ratio of In/Sn = 8–9, so the ITO thin film must be highly doped with tin and high degeneration can be realized, which is the origin of the carrier in the films. According to previous reports [1], the reflection in the infrared region is realized to be related with the carrier density in the ITO thin films.

The absorption spectra shown in Fig. 3(c) and (f) give useful information about the property of the thin films. As shown in the figures, the as-deposited films have much higher absorption than the high temperature annealed films. This could be the source of the low transparency of the as-deposited films. Comparing the films deposited with and without oxygen atmosphere, the former ones show relatively lower absorption in the whole spectral region.

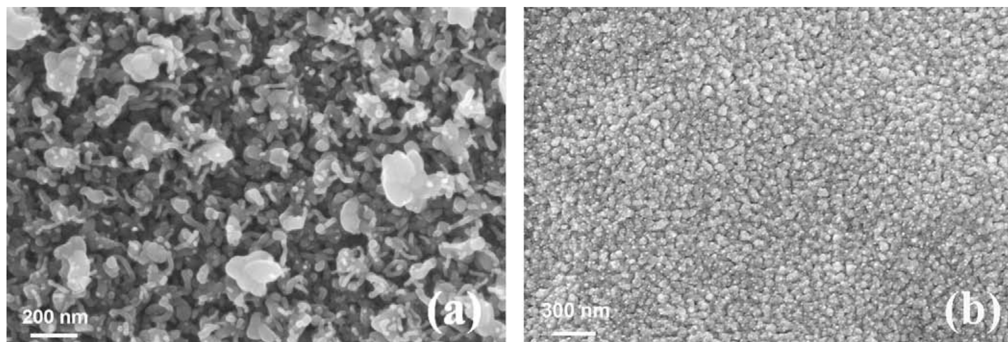

Fig. 1. FESEM images of the ITO thin film deposited without oxygen atmosphere (a), and with the oxygen pressure of 2.7×10^{-2} Pa (b).

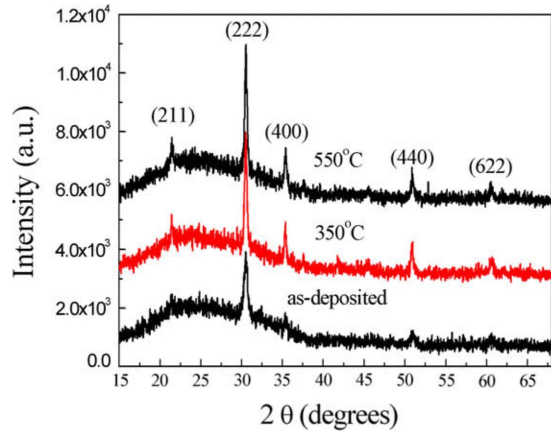

Fig. 2. XRD patterns of the as-deposited films fabricated under high oxygen pressure and annealed at different temperatures in N_2 atmosphere.

So the lower absorption of the films in this region can be attributed to the compensation of the oxygen during the deposition process, and the poor optical transmission in the as-deposited films is partly because of the oxygen deficiency. In addition to the high absorption of the as-deposited films, some fine structures can be identified in their absorption spectra as indicated by the arrows in the figures. Two broad shoulders are observed at around 570 and 1300 nm in Fig. 3(c) and (f) for the as-deposited films, which are disappeared after high temperature annealing. These two absorption shoulders can be ascribed to the oxygen deficiency or the oxygen deficiency related structure imperfection levels in the band-gap of ITO. Depositing film in oxygen rich atmosphere is favored for eliminating the structural defects, while post-annealing in high temperature is another effective method. All the films annealed at high temperature show low absorption, which can be due to the elimination of the defects. The perfection of the crystal structure can be also inferred from the XRD results as discussed above.

Fig. 4 shows the dependence of the sheet resistance on the annealing temperature under N_2 atmosphere for films deposited with and without oxygen. It is found that both films have the similar sheet resistance without annealing, but they show different tendency with the annealing temperature. For films deposited without oxygen, the sheet resistance firstly increases with elevating the annealing temperature up to 450 °C by more than three times, but after 550 °C annealing, the sheet resistance decreases abruptly. For films deposited under oxygen atmosphere, the sheet resistance firstly decreases with elevating the annealing temperature up to 350 °C by about three times, but further increasing the annealing temperature causes the increase of the sheet resistance. The lowest sheet resistance of about 25 Ω/□ (corresponding to 4.5×10^{-4} Ω cm) is obtained after 350 °C annealing.

4. Discussion

It is found that post-annealing can affect the film structures and in turn the properties strongly. Since the crystallization temperature of ITO film is as low as 200 °C, post-thermal annealing above 200 °C can improve the crystallinity of the films [13]. The structures of ITO will become more perfect after high temperature annealing, some grains can grow bigger by consuming the small grains around them and the number of grain boundaries is consequently reduced, which is helpful for reducing the resistance. The decrease of the resistance after annealed at 350 °C for the films deposited under oxygen atmosphere can be attributed to this effect. The improvement of the crystallinity will also give rise to the high optical transmission as a result of reducing light scattering at the grain boundary. Moreover, post-annealing can also eliminate the defects because of the improvement of the crystallinity in the films. Low concentration defect in ITO films are in some extend good for lowering the resistance of the film because high concentration defects will reduce the mobility of the carrier greatly and

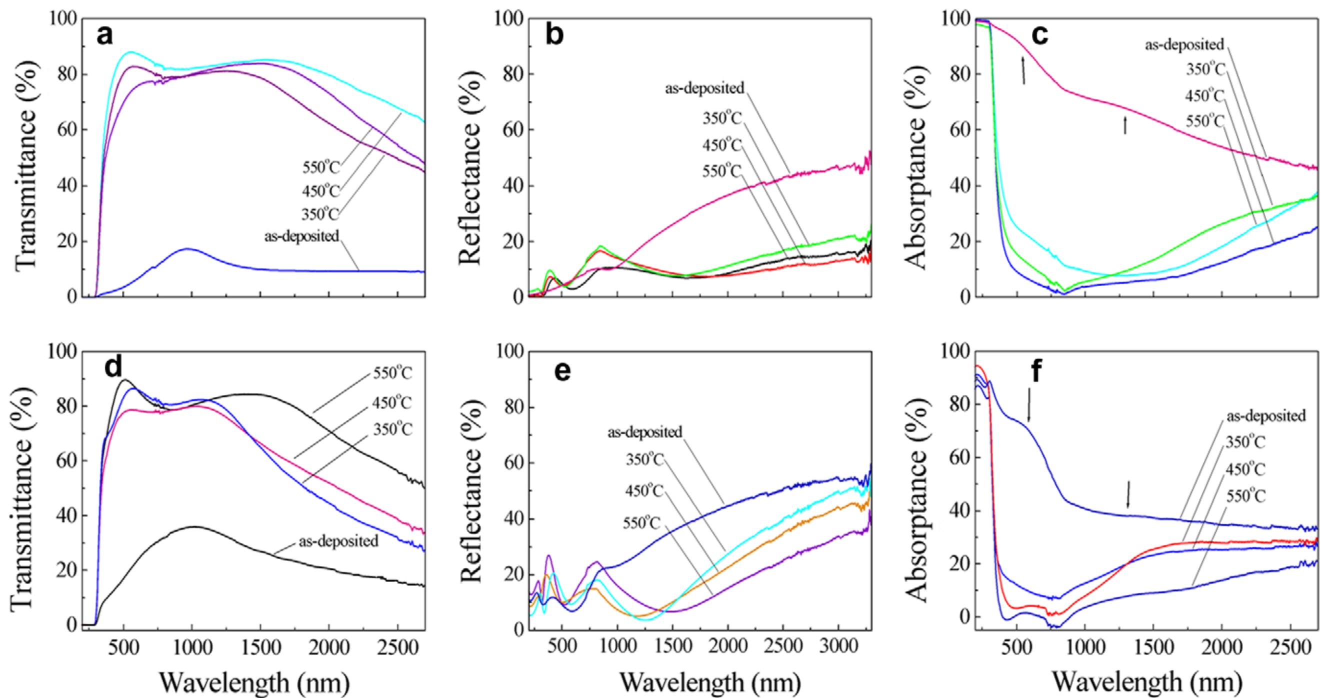

Fig. 3. Transmission spectra (a and d), reflection spectra (b and e), and the absorption spectra (c and f) for the films deposited without oxygen (a–c) and with the oxygen pressure of 2.7×10^{-2} Pa (d–f).

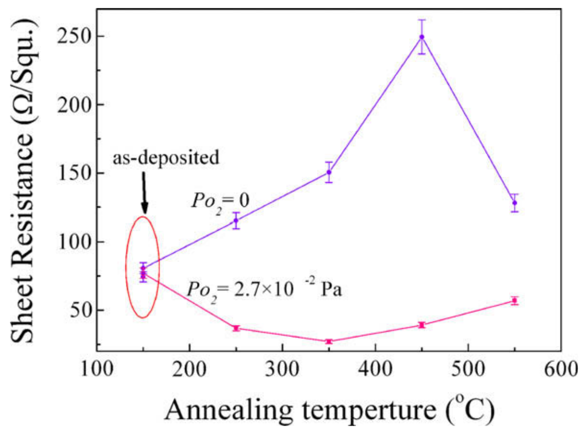

Fig. 4. Dependence of the sheet resistance on the annealing temperature for films deposited without oxygen and with the oxygen pressure of 2.7×10^{-2} Pa. The lines are drawn for guiding eyes.

decrease the optical transmission due to strong carrier-defect scattering and the optical absorption of the defect states. The oxygen vacancy and the oxygen deficiency defects are favored to be formed in the films deposited without or with low oxygen pressure, which is helpful for decreasing the resistance while is harmful for increasing the transparency. So it is always observed that the as-deposited film has the poorer transmission but the lower resistance than the film annealed at higher temperature. After high temperature annealing, the oxygen deficiencies will be eliminated gradually, which will contribute to the increase of the optical transmission and the resistance as seen in the 450 °C annealed films deposited without oxygen.

It is highly expecting to deposit ITO films as thin as possible while keeping good electrical, optical and mechanical properties. It is not only valuable for saving the source material, but is also favored for energy and time saving. The problems caused by reducing the film thickness are the increase in the sheet resistance and the decrease in mechanical strength of the films. In order to investigate the effect of the film thickness and to determine the optimum film thickness, ITO films with the thickness of about 45 nm were deposited under oxygen pressure of 2.7×10^{-2} Pa and substrate temperature of 150 °C. The optical transmission and absorption spectra of the films annealed at different temperature in N_2 is shown in Fig. 5(a) and (b). It is found that all the films show high transmission and low absorption in the whole measured spectral region, which is a little different from that shown in Fig. 3. This high transparency and low absorption can be ascribed to the ultrathin film thickness. Films annealed at high temperature also show the increased optical transmission and the decreased absorption, which is similar to the situation observed in Fig. 3.

The dependence of sheet resistance on the annealing temperature is presented in Fig. 5(c). For comparison, the sheet resistance of the films with the thickness of 180 nm is re-plotted in the same figure. It is shown that the sheet resistance of the films with thickness of 45 nm is much larger than that of 180 nm thin films. It is noted that the surface scattering will play a crucial role in the carrier transport process when the film thickness is comparable with the grain size in the film. Meanwhile, decreasing the film thickness greatly reduces the number of the possible conduction path connecting the adjacent grains. As demonstrated in Fig. 5(d), the path of the current is mediated by the effective electrical contact between the adjacent grains. More contact sites will result more effective current transport and lower sheet resistance. In the film with thickness several times larger than the grain size, the available current path is formed as the three-dimensional network, while in films with thickness comparable with the grain size, due to the reduced number of the contact sites, the available current path is limited only between two adjacent grains. Due to the reduced contact sites when the film thickness is comparable with the grain size, the effect of the surface scattering and the lack of

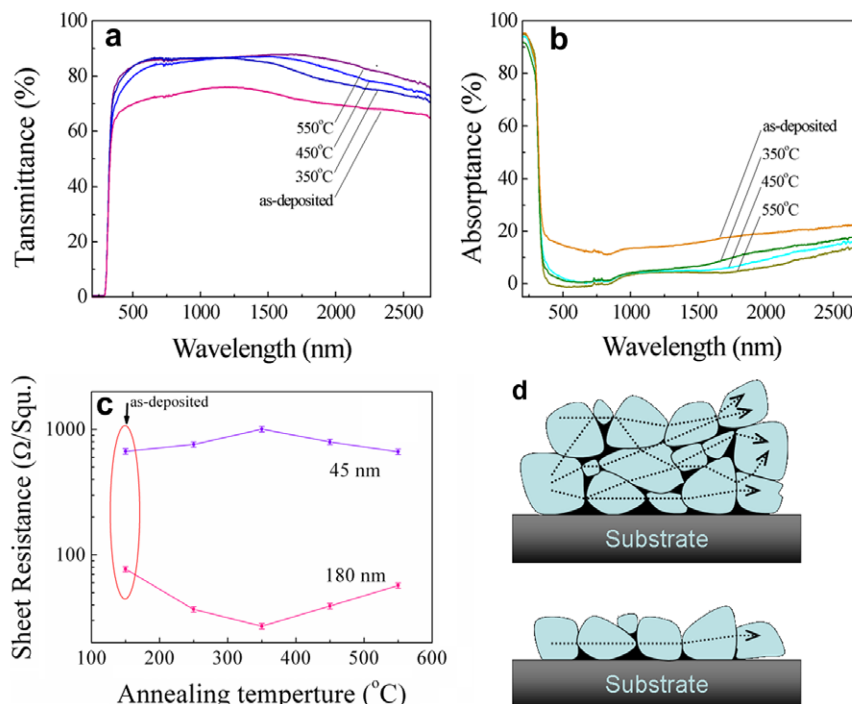

Fig. 5. Transmission (a) and absorption (b) spectra for 45-nm thick ITO thin films annealed at different temperatures in N_2 atmosphere, and (c) the dependence of the sheet resistance on the annealing temperature. The lines are drawn for guiding eyes. (d) The schematic figure shows the possible current path in the polycrystalline ITO thin films, (I) the film thickness is several times larger than the grain size. (II) The film thickness is comparable with the grain size.

Table 1
List of room temperature resistivity, transmittance (at 550 nm), and FOM of the ITO thin films in the current work and several previous reports by using different preparation methods.*

Method	Resistivity ($\times 10^{-4}\ \Omega$ cm)	Transmittance (%)	Film thickness (nm)	FOM ($\times 10^{-3}\ \Omega^{-1}$)	Reference
EBE	4.5	85	180	7.9	Current work
	10	80	20	0.89	[14]
	7.0	93	250	6.5	[7]
Sputtering	2.0	85	80	8.9	[15]
	2.4	85	160**	13.1	[16]
PLD	5.0	89	220	13.6	[4]
	4.0	80	317	8.3	[5]
Spray pyrolysis	8.0	85	160	3.9	[9]
	27	94	205	4.1	[10]
Sol–gel	20	Not given	125	–	[17]
	80	80	250	0.3	[18]

* Several data in the table were roughly obtained from the figures in the corresponding references.
** Average value.

conduction path will dominate the conduction of the thin films. According to the FESEM and XRD results, the grain size of the ITO film is about 30 nm, so the effect of surface scattering and the reduced conduction path is much more obvious in 45-nm thick ITO films than that in thicker samples which cause the large resistance. It can be concluded that the thickness of the ITO films used for TCO must be several times thicker than the dimension of the grain size in order to get better conductance.

It is well known that there is a compromise between electrical conductivity and optical transparency in ITO films [9,10]. They correlated with each other in factors such as film density, film thickness, defect density and grain size. Take the film density as example, densely packaged film shows better connectivity which results in better conduction path thus lower resistance, but it also results in films with higher refraction index that cause higher light reflection thus lower optical transmittance. The defect density also have dual effect: high defect density will cause severe optical absorption caused by the defect levels in the band-gap that give negative effect to the optical transmittance, but this kind of defect levels on the other hand serves as efficient conduction path in reducing the resistance of the film. Considering the above mentioned factors, it is very important to define the figure of merit (FOM) in order to interpretation the overall properties of the ITO films: [9,10]

$$\mathrm{FOM} = \frac{T^{10}}{R_s},$$

where T stands the transmittance and R_s is the sheet resistivity. In our optimized conditions, ITO thin films show typical resistivity of $4.5 \times 10^{-4}\ \Omega$ cm ($R_s = 25\ \Omega/\square$) and the optical transmittance of about 85% (at 550 nm), the FOM value is calculated to be $7.9 \times 10^{-3}\ \Omega^{-1}$, which can be estimated to be a good result comparing with the results reported previously as shown in Table 1. It is also noted in Table 1 that there is relatively less diversity in data of the optical transparency in ITO thin films deposited by using different preparation methods, but there is about one order of magnitude difference for the data of resistivity, which highlights the different deposition process on the key factor of quality in ITO thin films. According to Table 1, ITO thin films deposited by sputtering and PLD show more stable performance and the EBE method also show good results. By considering both the quality and the cost, the EBE method can be taken as a good choice for actual applications.

The ITO thin film deposited in the optimized conditions is used as the top electrode on the Si quantum dots/SiO_2 multilayer (SSM) light emitters. The detailed information on the multilayered structures preparation can be found elsewhere [19]. The 90 nm ITO is deposited onto the SSM sample by using a shadow mask with the diameter of 1.5 mm. The substrate temperature is 150 °C, the oxygen pressure is 2.5×10^{-2} Pa, and the deposition rate is 2 Å/s during deposition of the ITO top electrode. The sample is then annealed at 400 °C for half an hour under N_2 atmosphere after the ITO top electrode is deposited. The typical EL spectra and the current–voltage (I–V) relationship of the sample are shown in Fig. 6. As shown in the inserted figure, the current increases exponentially with increasing the applied voltage, which indicates the rectifying property of the metal–insulator–semiconductor (MIS) structure. The diode parameters of diode ideality factor and series resistance were extracted from the linear part in the forward biased In (I)–V curve by using the method introduced by Cheung and Cheung [20]. The typical diode ideality factor and series resistance were found to be 1.98 and 582 Ω, respectively. The diode have relatively large ideality factor and the series resistance, indicating that the SSM with high interface state works as an insulating layer between the metallic-like ITO and the p-Si substrate [21]. Another important effect which cannot be neglected is that our device emits light which evolves into the carrier generation and recombination process. Similar to the situation in the Al/SiO_2/p-Si MIS structure, it is also observed that the current rises slowly with the reverse bias and does not show any effect of saturation (data not shown), which can be explained in terms of the presence of the interfacial

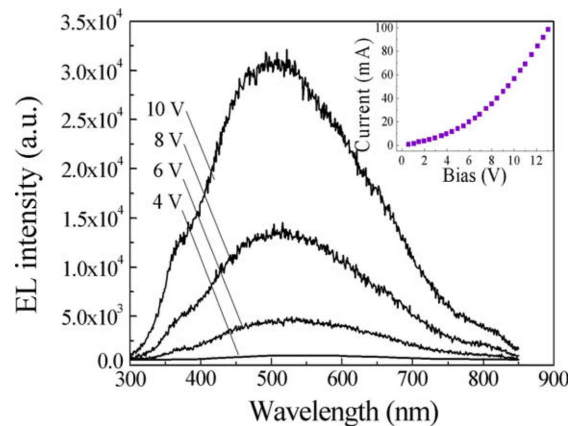

Fig. 6. EL spectra at different voltages for the EL devices containing Si QDs/SiO_2 multilayers by using ITO as the top electrode. Inset shows the I–V relationship of the devices.

insulator layer between the ITO and the p-Si substrate and the image force lowing of Schottky barrier height.

Based on the *I–V* curve of the ITO/SSM/p-Si structure, the nature of the metal–semiconductor contact sandwiched with an insulating layer can be inferred, which indicates a good compatibility of the EBE deposited ITO thin films used as the top electrode in the silicon-based light emitters. An intense electro-luminescence (EL) is observed by using the ITO top electrode. The broad peak centered at around 550 nm can be attributed to the recombination of carriers in nc-Si embedded in the SSM structures [19]. With increasing the applied voltage, the intensity increases gradually and the luminescence can be clearly observed visually in the dark room. The intense EL from the device further confirms that the ITO film deposited by EBE method under the optimized conditions is suitable for using as the high transparency and low resistance top electrode in the silicon-based opto-electronic devices.

5. Conclusion

ITO thin films were deposited by EBE method under different deposition processes. The effect of the deposition atmosphere, deposition temperature and the films thickness on the optical and electrical properties was studied. It is found that deposition in oxygen atmosphere is suitable for obtaining high quality ITO thin films with closely packaged microstructure and low density defects. Post-annealing can improve the optical transmission and influence the electric properties strongly by modifying the film structures and defects states. The 180-nm thick ITO films with the device quality is deposited under oxygen pressure of 2.7×10^{-2} Pa with the substrate temperature of 150 °C and post-annealed at 350 °C in N_2 atmosphere. The sheet resistance can be as low as 25 Ω/□ and the transmittance is about 85% at 550 nm. The ITO films deposited under the optimized conditions work well as the TCO electrode in the light emitting devices based on Si/SiO_2 multilayer containing Si quantum dots and a strong EL could be observed at room temperature.

Acknowledgements

This work is supported by “973” project (2007CB613401), NSF of China (No. 10874070, 60721063), NSF of Jiangsu province (BK2008253) and SRFDP (20070284020).

References

[1] I. Hamberg, C.G. Granqvist, J. Appl. Phys. 60 (1986) R123–R159.
[2] Daihua Zhang, Chao Li, Xiaolei Liu, Song Han, Tao Tang, Chongwu Zhou, Appl. Phys. Lett. 83 (2003) 1845–1847.
[3] Tadatsugu Minami, Shinzo Takata, Toshikazu Kakumu, J. Vac. Sci. Technol. A 14 (1996) 1689–1693.
[4] Cristian Viespe, Ionut Nicolae, Cornelia Sima, Constantin Grigoriu, Rares Medianu, Thin Solid Films 515 (2007) 8771–8775.
[5] V. Craciun, D. Craciun, Z. Chen, J. Hwang, R.K. Singh, Appl. Surf. Sci. 168 (2000) 118–122.
[6] Yanfa Yan, J. Zhou, X.Z. Wu, H.R. Moutinho, M.M. Al-Jassim, Thin Solid Films 515 (2007) 6686–6690.
[7] Hamid Reza Fallah, Mohsen Ghasemi, Ali Hassanzadeh, Hadi Steki, Mater. Res. Bull. 42 (2007) 487–496.
[8] H. Kim, A. Piqué, J.S. Horwitz, H. Mattoussi, H. Murata, Z.H. Kafafi, D.B. Chrisey, Appl. Phys. Lett. 74 (1999) 3444.
[9] M. Ait Aouaj, R. Diaz, A. Belayachi, F. Rueda, M. Abd-Lefdil, Mater. Res. Bull. 44 (2009) 1458–1461.
[10] A.V. Moholkar, S.M. Pawar, K.Y. Rajpure, V. Ganesan, C.H. Bhosale, J. Alloys Compd. 464 (2008) 387–392.
[11] R.P. Burns, G. Demaria, J. Drowart, M.G. Inghram, J. Chem. Phys. 38 (1962) 1035–1036.
[12] T. Neubert, F. Neumann, K. Schiffmann, P. Willich, A. Hangleiter, Thin Solid Films 513 (2006) 319–324.
[13] A.S.A.C. Diniz, C.J. Kiely, Renew. Energy 29 (2004) 2037–2051.
[14] N. Mori, S. Ooki, N. Masubuchi, A. Tanaka, M. Kogoma, T. Ito, Thin Solid Films 411 (2002) 6–11.
[15] M.G. Zebaze Kana, E. Centurioni, D. Iencinella, C. Summonte, Thin Solid Films 500 (2006) 203–208.
[16] C. Guillén, J. Herrero, Vacuum 80 (2006) 615–620.
[17] K. Daoudi, B. Canut, M.G. Blanchin, C.S. Sandu, V.S. Teodorescu, J.A. Roger, Thin Solid Films 445 (2003) 20–25.
[18] M.J. Alam, D.C. Cameron, Thin Solid Films 420&421 (2002) 76–82.
[19] D.Y. Chen, D.Y. Wei, J. Xu, P.G. Han, X. Wang, Z.Y. Ma, J. Chen, W.H. Shi, Q.M. Wang, Semicond. Sci. Technol. 23 (2008) 015013.
[20] S.K. Cheung, N.W. Cheung, Appl. Phys. Lett. 49 (1986) 85.
[21] A. Tataroğlu, S. Altındal, Microelectron. Eng. 85 (2008) 233–237.